END
DATE
FILMED

DTIC

MICROCOPY RESOLUTION TEST CHART

NATIONAL BUREAU OF STANDARDS-1963-A

R-2298

DAVIDSON
LABORATORY

Report SIT-DL-82-9-2298

September 1982

DESIGN OF PROPELLER DUCTS TO
REDUCE CAVITATION AND VIBRATION

by

T.R. Goodman
and
J.P. Breslin

DTIC
ELECTE
AUG 3 1 1983

A

STEVENS INSTITUTE
OF TECHNOLOGY

CASTLE POINT STATION
HOBOKEN, NEW JERSEY 07030

R-2298

83 08 30 170

REPORT DOCUMENTATION PAGE		READ INSTRUCTIONS BEFORE COMPLETING FORM
1. REPORT NUMBER SIT-DL-82-9-2298	2. GOVT ACCESSION NO.	3. RECIPIENT'S CATALOG NUMBER
4. TITLE (and Subtitle) Design of Propeller Ducts to Reduce Cavitation and Vibration		5. TYPE OF REPORT & PERIOD COVERED FINAL 1 March 1981-30 Sept. 1982
		6. PERFORMING ORG. REPORT NUMBER SIT-DL-82-9-2298
7. AUTHOR(s) T.R. Goodman J.P. Breslin		8. CONTRACT OR GRANT NUMBER(s) N00014-81-K-0230
9. PERFORMING ORGANIZATION NAME AND ADDRESS Davidson Laboratory Stevens Institute of Technology 711 Hudson St., Hoboken, N.J. 07030		10. PROGRAM ELEMENT. PROJECT, TASK AREA & WORK UNIT NUMBERS SR 023-01-01
11. CONTROLLING OFFICE NAME AND ADDRESS David W. Taylor Naval Ship Research and Development Center Bethesda, Maryland 20084		12. REPORT DATE September 1982
		13. NUMBER OF PAGES i,ii, 14 pgs. 2 Appendices, 4 Figures
14. MONITORING AGENCY NAME & ADDRESS(If different from Controlling Office) Office of Naval Research 800 N. Quincy St. Arlington, Va. 22217		15. SECURITY CLASS. (of this report) Unclassified
		15a. DECLASSIFICATION/DOWNGRADING SCHEDULE

16. DISTRIBUTION STATEMENT (of this Report)
Approved for Public Release:
Distribution Unlimited

17. DISTRIBUTION STATEMENT (of the abstract entered in Block 20, if different from Report)

18. SUPPLEMENTARY NOTES

Sponsored by the Naval Sea Systems Command, General Hydromechanics Research
Program, administered by the David W. Taylor Naval Ship and Development
Center, Code 1505, Bethesda, MD 20084.

19. KEY WORDS (Continue on reverse side if necessary and identify by block number)

Propeller Duct, Hydrodynamics

20. ABSTRACT (Continue on reverse side if necessary and identify by block number)

A procedure based or inviscid flow theory is detailed for the design of pro-
peller ducts to reduce specific spatial non-uniformities in given nominal
ship wakes. The objective is to produce net flows to enclosed propellers
which will reduce cavitation and vibratory forces. The process yields
peripherial variations of camber and conicity angle which will reduce the
amplitude of specific wake harmonics to a maximum extent possible under the
arbitrarily imposed constraint that the maximum sectional normal force

(over)

DD FORM 1473 EDITION OF 1 NOV 65 IS OBSOLETE
1 JAN 73
S/N 0102-014-6601

20. (Continued)

coefficient must not exceed unity. Applications are made to reduce the first shaft frequency of two wakes showing resultant first harmonics reduced by factors of 4 and 1.40 in the 0.8 radius region. A 9.5-inch diameter model designed to reduce the first shaft harmonic of a screen-generated wake has been constructed for experimental verification of the efficacy of the design. Computer programs are provided.

STEVENS INSTITUTE OF TECHNOLOGY
DAVIDSON LABORATORY
Castle Point Station, Hoboken, New Jersey 07030

Report SIT-DL-82-9-2298

September 1982

DESIGN OF PROPELLER DUCTS TO
REDUCE CAVITATION AND VIBRATION

by

T.R. Goodman

and

J.P. Breslin

Approved:

Daniel Savitsky
Acting Director

LIST OF SYMBOLS

a_i	coefficient multiplying rooftop distributions
c	semi-chord of the duct
C_ℓ	sectional list coefficient
C_p	pressure coefficient $(= p/\frac{1}{2}\rho U^2)$
g_m	see Equation (23)
h	height of rooftop pressure distribution
H_m	see Equation (20)
I_m	see Equation (5)
J_m	see Equation (24)
K_m	kernel function for calculating α_m (see Equation (29))
K_{x_m}	kernel function for calculating $y_m(x)$ (see Equation (34))
M	number of rooftop distributions used
p	pressure
$Q_{m-1/2}$	Legendre function of the second kind of order $m - 1/2$
r	radial coordinate
r_o	radius of the duct
R	Descarte distance
s	dummy radial coordinate (also radius of the duct)
u	axial perturbation velocity $(= \partial\phi/\partial x)$
U	forward speed of ship
x	axial coordinate
x_o	point at which rooftop pressure distribution begins to descend to zero
y_m	ordinates of camber line
Z	argument of Legendre functions - see Equation (6)
α_m	pitch angle of section
Y	tangential coordinate

i

Δ	jump
ε	a small quantity
ε_m	see below Equation (3)
θ	dummy tangential coordinate
ξ	dummy axial coordinate
ρ	mass density of fluid
ϕ	velocity potential

SUBSCRIPTS

c	calculated
i	index to distinguish different unit rooftop pressure distributions
j	index to distinguish different unit rooftop pressure distributions
m	harmonic order
me	measured

INTRODUCTION

It is proposed, and an analysis is developed, to design a non-axially-symmetric duct intended to shroud a propeller. One of the first experimental indications of the possible benefits to be secured from ducts having non-axially symmetric distributions of camber was given by Shpakoff and Turbal at the Twelfth ITTC in Rome, 1969[1]. Unfortunately, the official proceedings give only three curves which compare the variation in axial blade bending moment at the root of a model propeller operating behind a model of a tanker with a) no duct; b) symmetrical duct; c) non-symmetrical duct. The results show that the bending moment variations were much larger with the symmetrical duct than with no duct, and were greatly reduced by the duct with circumferentially distributed camber. This experience surely refutes the oft-repeated conception that a duct homogenizes the inflow. This trend is confirmed by calculations employing a program developed by Tsakonas, et al[2] which showed that vibratory thrust was predicted to be increased by 20 percent by a simple duct as compared to the ductless case.

In 1973, Turbal[3] advanced a theoretical method for calculating the shape of ducts which, in his terms, "rectifies" the wake flow. Turbal attempted to calculate a duct which annuls the total axial and tangential velocity nonuniformities. This is unnecessary if one desires merely to reduce the blade rate shaft thrust and torque as well as the transverse and vertical forces and moments about the horizontal and vertical axes. It is also unnecessary if one merely wishes to inhibit the onset of intermittent blade cavitation. With the first objective in mind, it is only necessary to calculate additive camber distributions which induce opposing spatial flows inside the duct at the $n-1$, n and $n+1$ harmonics (n being the blade number). With the second objective in mind, it is only necessary to calculate additive camber distributions which induce spatial flows opposing the lower order harmonics, say 1, 2 and 3. Since the Fourier harmonics are linearly independent and the theory presented is a linear one, it is possible to design a duct to achieve both objectives simultaneously. Turbal's analytical method does not allow any insight into the physics of the problem and appears to suffer from numerical instabilities.

1

In the next section, an analytical method, using linearized theory, is presented for calculating the circumferential camber distribution of a non-axially symmetric duct and to assess the amount by which the axial velocity which is present in the absence of the duct is reduced by the duct.

THEORY OF NON-AXIALLY SYMMETRIC DUCTS

We imagine a duct without a propeller immersed in the wake of a single screw ship or submarine, and limit our attention to wakes which have port-starboard symmetry (i.e., the ship is on a straight course; the submarine could be trimmed up or down, but not yawed). We seek to calculate a duct camber distribution which will induce axial flow components opposing those of the given wake over the locus of the disc of the propeller at spatial frequency m. (The frequency m may take on values of 1, 2, n-1, n, n+1, etc.) The camber distribution must be such that the kinematic boundary condition on the duct surface is satisfied. The unknowns are the camber distribution, as well as the pressure distribution on the duct, as functions of the chordwise and circumferential coordinates.

We begin by expressing the pressure field in cylindrical coordinates in terms of a pressure jump Δp on the cylindrical surface $s = r_o{}^*$:

$$p(x,r,\gamma) = \frac{1}{4\pi} \int_0^{2\pi} \int_{-c}^{c} \Delta p \frac{\partial}{\partial s} \left(\frac{1}{R}\right) s \, d\xi \, d\theta \tag{1}$$

where R is the Descarte distance between the fixed point (x,r,γ) and the dummy point (ξ,s,θ). In other words

$$\frac{1}{R} = \frac{1}{\{(x-\xi)^2 + r^2 + s^2 - 2rs \cos(\theta-\gamma)\}^{1/2}} \tag{2}$$

By expanding $1/R$ into a Fourier series in $\theta-\gamma$, it can be shown that

$$p(x,r,\gamma) = \frac{1}{4\pi^2} \sum_{m=0}^{\infty} \varepsilon_m \int_0^{2\pi} \int_{-c}^{c} \frac{\Delta p}{\sqrt{r}} \frac{\partial}{\partial s} \left[\frac{1}{\sqrt{s}} Q_{m-1/2}\left(\frac{(x-\xi)^2 + r^2 + s^2}{2rs}\right)\right] \cos m(\gamma-\theta) s \, d\xi \, d\theta \tag{3}$$

Because the only value of s in which we are interested is $s = r_o$, the two symbols will be used interchangeably.

where $\varepsilon_m = 1$ for $m = 0$

$= 2$ otherwise

$Q_{m-1/2}$ is the associated Legendre function of the second kind of half odd integer order. The properties of the Legendre function are given, for example, in Ref. 4.

Upon carrying out the indicated differentiation with respect to s, the field pressure becomes

$$p = \frac{1}{8\pi^2} \sum \frac{\varepsilon_m}{\sqrt{rs}} \int_0^{2\pi} \cos m(\gamma - \theta) d\theta \int_{-c}^{c} \Delta p(\theta, \xi) I_m d\xi \tag{4}$$

where

$$I_m = \{-Q_{m-1/2} + \frac{4rs(m+\frac{1}{2})[s^2 - r^2 - (x-\xi)^2]}{[(x-\xi)^2 + (r-s)^2][(x-\xi)^2 + (r+s)^2]} Q_{m+1/2} - Z\,Q_{m-1/2}\} \tag{5}$$

and the argument of all the Q functions is[*]

$$Z = \frac{(x-\xi)^2 + r^2 + s^2}{2rs} \tag{6}$$

If the pressure jump Δp is expressed as a Fourier series in θ,

$$\Delta p = \sum_{n=0}^{\infty} \Delta p_n(\xi) \cos n\theta \tag{7}$$

and the field pressure is also expressed as a Fourier series in γ,

$$p = \sum_{m=0}^{\infty} p_m(x,r) \cos m\gamma \tag{8}$$

Then, upon substituting (7) into (4) and carrying out the θ-integral, it can be shown, as a consequence of the orthogonality between the trigonometric functions, that

---

[*] *When $r = s$ and $\xi = x$, Z becomes unity and the Q functions are logarithmically infinite. Although this singularity is integrable, it offers problems in the numerical evaluation of the integrals which can be avoided altogether by taking the maximum value of r to be $s-\varepsilon$ where ε is a small quantity.*

$$p_m(x,r) = \frac{\varepsilon_m}{8\pi\sqrt{rs}} \int_{-c}^{c} \Delta p_m(\xi) \, I_m d\xi \tag{9}$$

As a consequence of the linearized Bernoulli equation

$$p = \rho U \frac{\partial \phi}{\partial x} \tag{10}$$

Equation (9) can be restated:

$$\left(\frac{1}{U}\frac{\partial \phi}{\partial x}\right)_m = \frac{\varepsilon_m}{16\pi\sqrt{rs}} \int_{-c}^{c} \Delta C p_m(\xi) \, I_m d\xi \tag{11}$$

where C_p is a pressure coefficient. Equation (11) gives a relationship between the axial flow inside the duct and the pressure jump across the duct sections for every Fourier component. If the pressure jump were known, the axial velocity could be calculated. It is our desire to choose a pressure jump such that the induced axial velocity nullifies, as much as possible, the nonuniformity of one or more Fourier components of the ship wake and that has shockless entry at the leading edge. Thus, Eq. (11) is, in fact, a Fredholm integral equation of the first kind to determine ΔC_{p_m} in terms of $(1/U \; \partial \phi/\partial x)_m$. Examination of the corresponding two-dimensional integral equation has disclosed that the solution is not unique. Presumably, the three-dimensional equation given here has the same property. If so, the property is advantageous because it means that there is more than one pressure distribution that will do the job.

The following method was originally proposed to solve Eq. (11):

We define a rooftop pressure distribution for the mth harmonic as follows:

$$\Delta C_p(\xi) = h, \qquad -c < \xi < x_o$$

$$\Delta C_p(\xi) = h\left(\frac{c-\xi}{c-x_o}\right), \; x_o < \xi < c \tag{12}$$

The lift coefficient on the section is then

4

$$C_\ell = \frac{1}{2C} \int_{-c}^{c} \Delta C_p \, d\xi = \frac{h}{4} [3 + \frac{x_o}{c}] \tag{13}$$

When $h = 1$, the resulting distribution is said to be a unit rooftop. We now consider several unit rooftops that differ only in the numerical value of x_o and distinguish them using the subscript i. The correct pressure distribution will consist of a linear sum of M of these unit rooftops weighted by unknown coefficients a_i. Thus,

$$\Delta C_p = \sum_{i=1}^{M} a_i \Delta C_{p_i} \tag{14}$$

Corresponding to each unit rooftop is a radial distribution of axia city at a specified station x designated as u_i. Thus

$$u_c(r) = \sum a_i u_i(r) \tag{15}$$

where the subscript c means that the velocity is calculated. We now consider a penalty function

$$I = \int_{o}^{s-\varepsilon} rdr \, [u_{me} - u_c]^2 \tag{16}$$

where the subscript me means that the velocity is measured. The weighting factor r is introduced to emphasize the outer radii of the duct where the propeller is most heavily loaded. We wish to determine u_c so that it equals u_m as best it can. We, therefore, minimize I with respect to each of the a_i's and set the minimum equal to zero. Upon substituting (15) into (16) and carrying out these operations, we are led to the following system of equations for the a_i's.

$$\int_{o}^{s-\varepsilon} rdr \, u_j u_m = \sum_{i=1}^{M} a_i \int_{o}^{s-\varepsilon} u_j u_i \, rdr \qquad 1 < j < M \tag{17}$$

The coefficients $\int_{o}^{s-\varepsilon} u_j u_i rdr$ form a symmetric matrix. Calculations of the u_i's and the matrix coefficients were carried out using Eq. (11) for five different unit rooftops with $x = 0$ and $x_o = -1.0, -0.6, -0.2, +0.2, +0.6$ leading to a five-by-five matrix. It was found that the matrix was highly ill-conditioned. This means that the axial flow in the duct is unable to distinguish one

5

unit rooftop from another or, put another way, that the shape of the
axial velocity profile in the duct is virtually the same regardless of
the shape of the pressure distribution on the duct. For this reason,
the concept of representing the pressure distribution on the duct by
several unit rooftops had to be abandoned. It was recognized that the
velocity profile in the duct is primarily dependent on the magnitude of
the total sectional lift and is insensitive to the shape of the distribu-
tion. Thus, we selected only one unit rooftop to represent ΔC_p. The one
chosen was for $x_o = +0.6$ and, in this case, the matrix equation (17) re-
duces to a single equation for $a_i = h$. The result is

$$
h = \frac{\int_o^{s-\varepsilon} r\,dr\; u_{me}\, u_i}{\int_o^{s-\varepsilon} r\,dr\; u_i^2}
\tag{18}
$$

Once h is determined in this way, the lift coefficient on the duct section
can be calculated using Eq. (13).

It is stated on page 529 of the paper by Van Manen and Oosterveld[5]
that the sectional lift on an axially symmetric duct should not exceed
unity at the risk of inducing stall. In our case, the lift varies circum-
ferentially, alternating between positive and negative values since it is
proportional to $\cos m\cdot$. Because the maximum lift is only experienced
locally as we proceed around the circumference, the Van Manen and
Oosterveld limitation may be too restrictive. However, it is certainly
a conservative limitation and, in the absence of any other criterion, we
will use it.

Now, the lift coefficient calculated using Eqs. (18) and (13) may
be smaller or greater than unity. If it is greater than unity, it must
be reduced to unity in accordance with our criterion and the value of h
must be correspondingly reduced. This means that the duct can be expected
to cancel the mth harmonic of the measured axial velocity only partially.

We present now an example of how a duct may be expected to affect
the axial flow. For the example, only the first harmonic of a wake will
be considered. The data is taken from Figure 27 of Hadler and Cheng[6]
which is reproduced here as Figure 1. Only the data for the first harmonic
and Model 4602, indicated by circles, will be considered. The chord of

6

the duct is taken to be equal to the radius (s = 2); the section where the first harmonic is to be rectified is the midsection (x = 0); the rooftop distribution begins to fall off at 0.8 of the chord (x_o = .6). Then $C_{\imath}$, as calculated using Eqs. (18) and (13) becomes $C_{\imath}$ = .9766, which is within the Van Manen and Oosterveld limitation. A plot of the data from Figure 1 is reproduced in Figure 2, together with the modified wake harmonic to be expected with the duct in place. It can be seen that the large velocities at the outer radii have been significantly reduced. At the inner radii, the negative velocities have become more negative. On the other hand, it is well known that intermittent cavitation occurs primarily at the outer radii where the bulk of the blade loading takes place, and so the beneficial effects of reducing the axial velocity at the outer radii should more than compensate for the deleterious effects of increasing the axial velocity at the inner radii.

It is the ultimate purpose of this project to design and build a duct according to the precepts set forth here. Consequently, a series of wind tunnel measurements taken behind a wake screen were carried out at the Princeton wind tunnel by Professor R. Hires. The screen was designed to simulate the flow in a ship wake. Details of the experiments will be presented in a subsequent report. For present purposes, we present only the result of the amplitudes of the first harmonic of the measured wake[*]. This is shown in Figure 3. The results of carrying out the computations indicated by Eqs. (18) and (13) show that $C_{\imath}$ = 3.0. Since this exceeds the Van Manen and Oosterveld limit, $C_{\imath}$ was reduced to unity and the modified wake with the duct in place is also shown in Figure 3. It can be seen that the modification created by the duct is a smaller percent of the total in this case than it was for the Hadler and Cheng wake previously analyzed. This is because the lift coefficient had to be reduced to unity in accordance with the Van Manen and Oosterveld limitation.

THE GEOMETRY OF THE DUCT SECTIONS

Up to this point we have examined the effect of a duct rooftop load distribution on the flow inside the duct. At this juncture, we

---

[*] *The phase varies slightly from radius to radius even though the wake screen is presumably symmetric. The duct cannot be expected to follow this radial variation in phase.*

determine the geometry of the duct for the same load distribution.

The starting point for our investigation of the geometry is Eq. (11). Upon differentiating with respect to r and simplifying, we find

$$\left(\frac{1}{U}\frac{\partial^2 \phi}{\partial r \partial x}\right)_m = \frac{\varepsilon_m/2}{8\pi}\int_{-c}^{c}\Delta C_{p_m}(\xi)\ H_m(x-\xi)\ d\xi \tag{19}$$

where

$$H_m(x-\xi) = \frac{1}{s^2(Z+1)}\ \{\frac{Z+1}{2}\ Q_{m-1/2}\ +$$

$$2(m+1/2)\ [\frac{(Z-3)Q_{m+1/2} - (Z^3 - 4Z+1)Q_{m-1/2}}{Z^2 - 1} + \overline{Q}_{m+1/2} - Z\overline{Q}_{m-1/2}]\}$$

$$\overline{Q}_{m-1/2} = \frac{(m+\frac{1}{2})}{Z+1}\ [Q_{m+1/2} - Z\ Q_{m-1/2}] \tag{20}$$

$$\overline{Q}_{m+1/2} = \frac{(m+\frac{3}{2})}{Z+1}\ [Q_{m+3/2} - Z\ Q_{m+1/2}]$$

We let c = 1 so that the unit of measure is the half-chord of the duct, and integrate Eq. (19) with respect to x from far upstream where all disturbances vanish.

$$\left(\frac{1}{U}\frac{\partial \phi}{\partial r}\right)_m = \frac{\varepsilon_m/2}{8\pi}\int_{-\infty}^{x}dx'\int_{-1}^{+1}\Delta C_{p_m}(\xi)\ H_m(x'-\xi;r)d\xi \tag{21}$$

Let t = x−x'. Then

$$\left(\frac{1}{U}\frac{\partial \phi}{\partial r}\right)_m = \frac{\varepsilon_m/2}{8\pi}\int_{0}^{\infty}dt\int_{-1}^{1}\Delta C_{p_m}\ H_m(x-t-\xi)d\xi \tag{22}$$

On interchanging the order of integration,

$$\left(\frac{1}{U}\frac{\partial \phi}{\partial r}\right)_m = \frac{\varepsilon_m/2}{8\pi}\int_{-1}^{+1}\Delta C_{p_m}(\xi)\ J_m(x-\xi)d\xi \equiv g_m(x) \tag{23}$$

where

$$J_m(x) = \int_{0}^{\infty}H_m(x-t)dt \tag{24}$$

8

Now consider the linearized boundary condition on the duct. This is that $1/U \, \partial \psi/\partial r$ = slope of the duct at $r = s$. Now, the slope consists of two parts, one due to the pitch, γ_m, of the section, and the other due to the slope of the camber line. Thus, if the camber line is defined as $v_m(x)$, the boundary condition is

$$\left(\frac{1}{U}\frac{\partial \psi}{\partial r}\right) = \gamma_m + v_m'(x) \tag{25}$$

Then Eq. (23) becomes

$$v_m'(x) = \gamma_m + q_m(x) \tag{26}$$

Upon integrating with respect to x from the leading edge where, by definition, $v(0) = 0$, we obtain

$$v_m(x) = \gamma_m(x+1) + \int_{-1}^{x} q_m(x')dx' \tag{27}$$

We define v_m to be zero at the trailing edge also, so that, upon setting $x = +1$, we obtain the following expression for γ_m

$$\gamma_m = -\frac{1}{2}\int_{-1}^{1} q_m(x')dx' \tag{28}$$

Substituting for $q_m(x')$ from Eq. (23) and interchanging the order of integration

$$\gamma_m = -\frac{\gamma_m/2}{16}\int_{-1}^{1} C_{p_m} K_n(\cdot) d\cdot \tag{29}$$

where

$$\chi(\cdot) = \int_{-1}^{1} J_n(x-\cdot) dx \tag{30}$$

using the definition of J_m, Eq. (24), and letting $u = t - x$, we find

$$\chi(\cdot) = \int dx \int H_m(u)du \tag{31}$$

9

This double integral can be manipulated into two single integrals as shown in Appendix A. The result is

$$K_m(\xi) = \int_{-(1-\xi)}^{1+\xi} (1+u-\xi)\, H_m(u)\,du + 2 \int_{1+\xi}^{\infty} H_m(u)\,du \tag{32}$$

The point $u = 0$ must be excluded because the integrand is singular in the Mangler sense. The final result, ready for numerical computation, is

$$K_m(\xi) = \int_{-(1-\xi)}^{-\epsilon}(1+u-\xi)H_m(u)\,du + \int_{\epsilon}^{1+\xi}(1+u-\xi)H_m(u)\,du + 2\int_{1+\xi}^{\infty}H_m(u)\,du - \frac{4}{\epsilon}(1-\xi) \tag{33}$$

where ϵ is a small quantity.

To summarize the computation of α_m, it is determined from Eq. (29) with $K(\xi)$ given by Eq. (33) and $H_m(u)$ given by Eq. (20) with $Z = 1 + u^2/2s^2$. Moreover, the kernel $K(\xi)$ is logarithmically singular at $\xi = \pm 1$ and, although these singularities are integrable, they present problems in numerically calculating the integral in Eq. (29). The problems can be avoided by changing the limits on the integral in Eq. (29) from ± 1 to $\pm(1-\epsilon)$ where ϵ is a small quantity.

In a similar manner, from Eq. (27) we can obtain an expression for the ordinates of the camber line with α_m considered to be known.

$$y_m - \alpha_m(1+x) = \frac{\epsilon_m/2}{8\pi} \int_{-1}^{1} \Delta C_{p_m}(\xi)\,d\xi\, K_{x_m}(\xi) \tag{34}$$

where

$$K_{x_m}(\xi) = \int_{-1}^{x} J_m(x_1-\xi)\,dx_1 \tag{35}$$

or, using the definition of J_m, Eq. (24), and letting $u = t - x$

$$K_{x_m}(\xi) = \int_{-1}^{x} dx_1 \int_{\xi-x_1}^{\infty} H_m(u)\,du \tag{36}$$

In a manner similar to that presented in Appendix A, the order of integration can be interchanged, the x_1 integral can be carried out, and the final result is

10

$$K_{x_m} = \int_{\xi-x}^{1+\xi} H_m(u)\,[x+u-\xi]\,du + (1+x)\int_{1+\xi}^{\infty} H_m(u)\,du \qquad (37)$$

$$\xi > x$$

$$K_{x_m} = \int_{-(x-\xi)}^{-\epsilon} H_m(u)\,[x+u-\xi]\,du + \int_{\epsilon}^{1+\xi} H_m(u)\,[x+u-\xi]\,du$$

$$+ (1+x)\int_{1+\xi}^{\infty} H_m(u)\,du - \frac{4}{\epsilon}(x-\xi) \qquad (38)$$

$$\xi < x$$

where, again, ϵ is a small quantity.

To summarize, the ordinates of the camber line are given by Eq. (34) where K_{x_m} is defined by Eqs. (37) and (38) and $H_m(u)$, Z, α_m are defined as before. Once again, the kernel K_x is logarithmically singular at $\xi = -1$ and $\xi = x$. The singularity can be avoided by changing the lower limit in Eq. (34) to $-(1-\epsilon)$ and surrounding the point $\xi = x$ by a small interval which is excluded from the integration scheme.

THE RESULTS OF SOME NUMERICAL COMPUTATIONS[*]

The value of α_m for several values of m were calculated for the case $s=1$, $x=0$, $x_o=0.6$. The results, together with one isolated case with $s=2$, are shown in Table 1.

Table I.   Values of α_m

	α_m/C_ℓ (s-1)	α_m/C_ℓ (s=2)
1	0.2912	0.1563
2	0.5607	N.A.
3	0.8322	N.A.
4	1.1038	N.A.
5	1.3356	N.A.

It can be seen that, as m increases, the angle α_m increases, and this means that the duct section must work harder and harder to produce the necessary axial flow to cancel a unit wake inflow. Fortunately, the magnitude of the wake inflow as the order of the harmonic increases tends

---

[*] A subroutine for calculating the Legendre functions was developed based on a series given in Reference 4 for $1 < Z \leq 1.09$ and based on a standard hypergeometric series for $Z \geq 1.09$.

to get smaller and smaller so that, in practice, the higher harmonics can usually be dealt with without exceeding the Van Manen and Oosterveld limit.

The cases $m = 1$, $s = 1,2$ indicate that a greater value of C_ℓ is required for the case $s = 2$ (chord - radius) than for the case $s = 1$ (chord = diameter) to achieve the same axial flow in the duct, and this is intuitively correct.

Points on the camber line for the case $m = 1$, $s = 2$ were calculated and are shown in graphical form in Figure 4 and in tabular form in Table II. These points were fitted to a polynominal passing through the points $(1,0)$ and $(-1,0)$ using a least square fit, and the resulting polynomial is

$$\frac{y_1}{C_\ell} = (1-x^2) \left[a_0 + a_1 x + a_2 x^2 + a_3 x^3 + a_4 x^4 \right] \tag{39}$$

where $a_0 = 0.15577$

$a_1 = -0.01669$

$a_2 = 0.05212$

$a_3 = -0.05540$

$a_4 = -0.03812$

It should be pointed out that, because we are dealing here with the first harmonic, Eq. (39) must be multiplied by $\cos\theta$, and also that α_1 must be multiplied by $\cos\theta$. Thus, both the camber and pitch angle vary circumferentially. Since the sections are at $\alpha_1 \cos\theta$, this effect can be achieved simply by tilting the complete duct at angle α_1. For all higher harmonics no such simple recourse is available, and the local pitch angle must be built into the duct.

It is because of the relative simplicity of the first harmonic that the Princeton tests and the computations carried out thus far have concentrated on this case. The ultimate purpose will be to build a duct based on the camber line of Eq. (9), to tilt it at the angle $\alpha_1 = .1563$, according to Table I, and to mount it in the Princeton tunnel behind the same wake screen as used in the preliminary tests and then, by taking measurements inside the duct, to prove the efficacy of a non-axially symmetric duct by demonstrating a reduction in the first harmonic of the

12

wake as shown theoretically in Figure 3. Such a duct is shown schematically in Figure 5.

CONCLUSIONS

A theory for the behavior and design of non-axially symmetric ducts intended to shroud a propeller is presented. Measured wake data is also presented, together with the modification of the wake caused by an appropriately designed duct. Moreover, the shape of such a duct is calculated for one case. It remains to build a model of such a duct and measure the modified wake inside it to demonstrate the tenets of the theory, and also to show that non-axially symmetric ducts can be expected to be useful in ameliorating transient propeller cavitation and vibratory shaft forces. The results of this ongoing program will be presented in a subsequent report.

ACKNOWLEDGMENT

The authors would like to thank Mr. Thomas McKay who prepared all the computer programs.

REFERENCES

1. Shpakoff, V.S. and Turbal, V.K.: "Method of Investigation into Efficiency of Axi-Symmetric and Non-Axisymmetric Ducts in Self-Propeller Models". Proceedings Twelfth International Towing Tank Conference, Rome, September 1969

2. Tsakonas, S., Jacobs, W.R. and Ali, M.R.: "Propeller Duct Interaction Due to Loading and Thickness Effects" Davidson Laboratory Report SIT-DL-75-1722, April 1975. Presented at the "Propeller 78" Symposium, Virginia Beach, Va., May 1978

3. Turbal, V.K.: "Theoretical Solution of the Problem on the Action of a Non-Axisymmetrical Ducted Propeller System in a Non-Uniform Flow". Symposium on Ducted Propellers, The Royal Institution of Naval Architects, London, 1973

4. Sluyter, Marshall M.: "A Computational Program and Extended Tabulation of Legendre Functions of Second Kind and Half Order" Therm Advanced Research Technical Report 601, Ithaca, N.Y., August 1960

5. Van Manen, J.D. and Oosterveld, M.W.C.: "Analysis of Ducted Propeller Design" SNAME Transactions, Vol. 74, pp. 522-562, 1966

6. Hadler, Jacques B. and Cheng, Henry M.: "Analysis of Experimental Wake Data in Way of Propeller Plane of Single and Twin-Screw Ship Models" SNAME Transactions, pp. 287-414, Vol. 73, 1965

TABLE II*

POINTS ON THE CAMBER LINE OF THE DUCT
TO BE USED IN PRINCETON WIND TUNNEL TESTS

x	y/c_2
.9	.0280361
.8	.0564023
.7	.0847943
.6	.109061
.5	.126248
.4	.138521
.3	.146653
.2	.153209
0	.156918
-.2	.150040
-.3	.143592
-.4	.134574
-.6	.107941
-.8	.0682754

---

*Referred to on page 13 of text.

APPENDIX A
REDUCTION OF THE DOUBLE INTEGRAL

$$K_m(\xi) = \int_{-1}^{1} dx \int_{\xi-x}^{\infty} H_m(u)\,du$$

In the u,x plane, the integral is carried out over the shaded region defined by the sketch below:
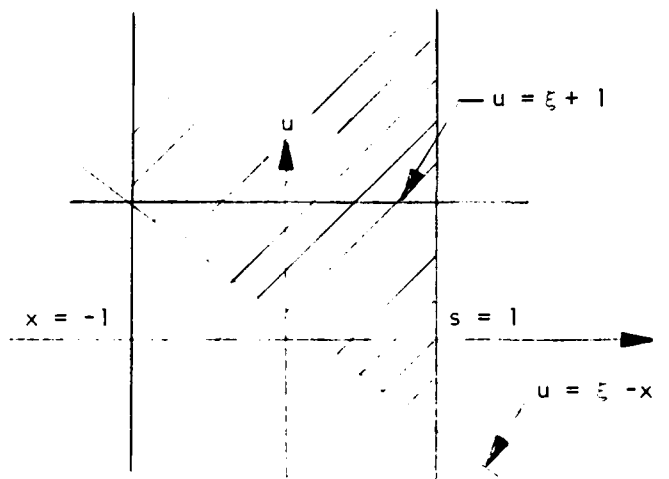
If the order of integration is changed, we must integrate on x first. Thus, we integrate over the triangle defined by the lines $u = \xi - x$, $u = \xi + 1$, $x = +1$, and then add the integral over the semi-infinite rectangle defined by the lines $u = \xi + 1$, $u = \infty$, $x = \pm 1$. The result is

$$K_m(\xi) = \int_{-(1-\xi)}^{(1+\xi)} H_m(u)\,du \int_{\xi-u}^{1} dx + \int_{1+\xi}^{\infty} H_m(u) \int_{-1}^{+1} dx$$

After the x-integrals have been carried out, the result is Eq. (32).

APPENDIX B

COMPUTER PROGRAMS

The five computer programs that were used in the numerical computations are presented herein, together with descriptions of what they do and with a dictionary for each, relating Fortran variables to analytic variables for input and output statements.

PROGRAM 1

Calculates α/C_L for given m, s, x_o

	FORTRAN VARIABLE	ANALYTIC VARIABLE	DESCRIPTION
	S	s	
	M	m	
	XO	x_o	
	A		Lower limit of outer integral
Input	B		Upper limit or outer integral
	AERR		Absolute error tolerance for outer intrgral
	RERR		Relative error tolerance for outer integral
	EPSK	ε	Lower limit of certain inner integrals
	AERRK		Absolute error tolerance for inner integral
	RERRK		Relative error tolerance for inner integral
	ALPHA	α/C_L	
Output	CK		Value of outer integral

```
      EXTERNAL FK2
      COMMON S,M,Q
      COMMON/COMQ1/CQ(5,3,3),AQ(3),A2Q,BQ(3),GQ(3),
     1  A1Q(3),A3Q(3),EQ(3),B1Q(3),B3Q(3),FAC(3)
      COMMON/COMQ2/AQ22(6,3),BQ22(6,3)
      COMMON/COMFT/DQ(3),SQ,AMB
      COMMON/COMK2/XB,C,CL,EPSK,AERRK,RERRK
      COMMON/COMI/LC1,LC2,LC3,LC4,LC5
      LC1=0
      LC2=0
      LC3=0
      LC4=0
      LC5=0
      READ(5,901) S,M,XB
901   FORMAT(F,I,F)
      READ(5,902) A,B,AERR,RERR
902   FORMAT(4F)
      READ(5,902) EPSK,AERRK,RERRK
      CALL UERSET(1,LEVL)
      SQ=S*S
      PI=3.1415927
      Q=1.
      C=1.
      CL=1.
      CALL QCONST
      CK=FCADRE(FK2,A,B,AERR,RERR,ERR,IER)
      PX=1./(16.*PI*Q)
      ALPHA=PX*CK
      WRITE(6,903) ALPHA,CK
903   FORMAT(1X,'ALPHA = ',E14.6,2X,'CK = ',E14.6)
      END
```

```
      FUNCTION FK2(G)
      EXTERNAL FT,FT1,FT2
      COMMON S,M,G1
      COMMON/COMG1/CG(500,3),AQ(3),A2Q,BQ(3),GQ(3),
     1  A1G(3),A3Q(3),EQ(3),B1G(3),B3G(3),FAC(3)
      COMMON/COMQ2/AQ22(6,3),BQ22(6,3)
      COMMON/COMFT/DQ(3),SQ,AMJ
      COMMON/COMK2/XJ,C,CL,EPSK,AERRK,RERRK
      COMMON/COM1/LC1,LC2,LC3,LC4,LC5
      LC5=LC5+1
      G1=G
      A1=EPSK
      B1=1.-G
      A2=EPSK
      B2=1.+G
      A3=1.+G
      B3=12.5*S
      AERR=AERRK
      RERR=RERRK
      FK1=0.
      IF (G.EQ.1.) GO TO 11
      C1=DCADRE(FT1,A1,B1,AERR,RERR,ERROR,IER)
      C2=DCADRE(FT2,A2,B2,AERR,RERR,ERROR,IER)
      C3=DCADRE(FT,A3,B3,AERR,RERR,ERROR,IER)
      FK1=C1+C2+2.*C3-4.*(1.-G)/EPSK
   11 CONTINUE
      H=4.*CL/(3.+XJ/C)
      IF(-C.LT.G.AND.G.LE.XJ) DP=H
      IF(XJ.LT.G.AND.G.LT.C) DP=H*(C-G)/(C-XJ)
      FK2=FK1*DP
      RETURN
      END
```

```
      FUNCTION FT(T)
      COMMON S,M,GGGG
      COMMON/COMFT/DQ(3),SQ,AMU
      COMMON/COM1/LC1,LC2,LC3,LC4,LC5
      LC2=LC2+1
      DEL=T*T/(2.*SQ)
      Z=DEL+1.
      Z1=Z+1.
      ZQ=Z*Z
      DEL2=DEL*DEL
      IF(DEL.GE.0.09) GO TO 11
      IF(DEL.LT.1.E-7) GO TO 9
      Q1=QQ2(DEL,1)
      Q2=QQ2(DEL,2)
      Q3=QQ2(DEL,3)
      QPR1=DQ(2)/(2.+DEL)*(Q2-(1.+DEL)*Q1)
      QPR2=DQ(3)/(2.+DEL)*(Q3-(1.+DEL)*Q2)
      FT=1./(SQ*(2.+DEL))*((2.+DEL)/2.*Q1+
     1   2.*DQ(2)*((-2.+DEL)*Q2+(2.+DEL-DEL2*(3.+DEL))*Q1)/
     1   ((2.+DEL)*DEL)+QPR2-(1.+DEL)*QPR1)
      RETURN
    9 CONTINUE
      FT=1./(2.*SQ)*((FM*FM-.75)*ALOG(DEL)+2./DEL)
      RETURN
   11 CONTINUE
      Q1=QQ1(Z,1)
      Q2=QQ1(Z,2)
      Q3=QQ1(Z,3)
      QP1=DQ(2)/Z1*(Q2-Z*Q1)
      QP2=DQ(3)/Z1*(Q3-Z*Q2)
      FT=1./(SQ*Z1)*(Z1/2.*Q1+2.*DQ(2)*(((Z-3.)*Q2-
     1   (ZQ*Z-4.*Z+1.)*Q1)/(ZQ-1.)+QP2-Z*QP1))
      RETURN
      END
CC
      FUNCTION FT1(T)
      COMMON S,M,G
      COMMON/COM1/LC1,LC2,LC3,LC4,LC5
      LC1=LC1+1
      FT1=(1.-T-G)*FT(T)
      RETURN
      END
CC
      FUNCTION FT2(T)
      COMMON S,M,G
      COMMON/COM1/LC1,LC2,LC3,LC4,LC5
      LC1=LC1+1
      FT2=(1.+T-G)*FT(T)
      RETURN
      END
```

PROGRAM 2

Calculate $Y(x)/C_L$ for given m, 3, x_o, α/C_L

	FORTRAN VARIABLE	ANALYTIC VARIABLE	DESCRIPTION
	s	s	
	M	m	
	XX	x	
	XO	x_o	
Input	ALPA	α/C_L	
	A		Lower limit of first outer integral
	B		Upper limit of second outer integral
	AERR		Absolute error tolerance for outer integral
	RERR		Relative error tolerance for outer integral
	EPS	ε	Integrate from A to XX-EPS and from XX + EPS to B
Output	YY	Y/C_L	
	ALPA	$\imath/C_L$	
	CK		Sum of 1st and 2nd integrals
	CK1		1st Integral
	CK2		2nd integral

```
          EXTERNAL FK2
          COMMON S,M,G
          COMMON/COMG1/CG(6,3),AG(3),A2G,BG(3),SG(3),
     1     A1G(3),A3G(3),EG(3),F1G(3),B3G(3),FAC(3)
          COMMON/COMG2/AG22(6,3),SG22(6,3)
          COMMON/COMFT/DG(3),SG,AMG
          COMMON/COMK2/XG,C,CL
          COMMON/COM1/LC1,LC2,LC3,LC4,LC5
          COMMON/COMXX/XX
          LC1=0
          LC2=0
          LC3=0
          LC4=0
          LC5=0
          READ(5,901) S,M,XX,XG,ALPHA
  901     FORMAT(F,I,3F)
          READ(5,902) A,B,AERR,RERR,EPS
  902     FORMAT(5F)
          CALL UERSET(1,LEVL)
          SG=S*S
          PI=3.1415927
          G=1.
          A1=A
          B1=XX-EPS
          A2=XX+EPS
          B2=B
          C=1.
          CL=1.
          CALL QCONST
          CK1=FCADRE(FK2,A1,B1,AERR,RERR,ERR,IER)
          WRITE(6,90033) CK1
 90033    FORMAT(1X,E14.6)
          CK2=FCADRE(FK2,A2,B2,AERR,RERR,RERR,ERR,IER)
          CK=CK1+CK2
          PX=1./(8.*PI*G)
          YY=PX*CK-ALPHA*(XX+1.)
          WRITE(6,903) YY,ALPHA,CK,CK1,CK2
  903     FORMAT(1X,'Y = ',E14.6,2X,'ALPHA = ',E14.6,2X,
     1     /1X,'CK = ',3E14.6)
          END
```

```
      FUNCTION FK2(G)
      EXTERNAL FT,FT1,FT2
      COMMON S,M,G1
      COMMON/COMG1/CG(500,3),AG(3),A2G,BG(3),GG(3),
     1  A1G(3),A3G(3),SG(3),B1G(3),B3G(3),FAC(3)
      COMMON/COMG2/AG22(6,3),BG22(6,3)
      COMMON/COMFT/DG(3),SG,AMG
      COMMON/COMK2/XG,C,CL,EPSK
      COMMON/COM1/LC1,LC2,LC3,LC4,LC5
      COMMON/COMXX/XX
      LC5=LC5+1
      G1=G
      SINFIN=12.5*G
      A11=EPSK
      B11=XX-G
      A12=EPSK
      B12=1.+G
      A13=1.+G
      B13=SINFIN
      A22=G-XX
      B22=1.+G
      A23=1.+G
      B23=SINFIN
      AERR=0.
      RERR=.0001
      FXX=1.+XX
      FK1=0.
      IF (G.EQ.1.) GO TO 11
      IF(G.GT.XX) GO TO 111
      C1=DCADRE(FT1,A11,B11,AERR,RERR,ERROR,IER)
      C2=DCADRE(FT2,A12,B12,AERR,RERR,ERROR,IER)
      C3=DCADRE(FT,A13,B13,AERR,RERR,ERROR,IER)
      FK1=C1+C2+FXX*C3-4.*(XX-G)/EPSK
      GO TO 11
111   CONTINUE
      C1=DCADRE(FT2,A22,B22,AERR,RERR,ERROR,IER)
      C2=DCADRE(FT,A23,B23,AERR,RERR,ERROR,IER)
      FK1=C1+FXX*C2
11    CONTINUE
      H=4.*CL/(3.+XG/C)
      IF(-C.LT.G.AND.G.LE.XG) DP=H
      IF(XG.LT.G.AND.G.LT.C) DP=H*(C-G)/(C-XG)
      FK2=FK1*DP
      RETURN
      END
```

```
      FUNCTION FT(T)
      COMMON S,M,GGGG
      COMMON/COMFT/DQ(3),SQ,AM0
      COMMON/COM1/LC1,LC2,LC3,LC4,LC5
      LC2=LC2+1
      FM=M
      DEL=T*T/(2.*SQ)
      Z=DEL+1.
      Z1=Z+1.
      ZQ=Z*Z
      DEL2=DEL*DEL
      IF(DEL.GE.0.09) GO TO 11
      IF(DEL.LT.1.E-7) GO TO 9
      Q1=QG2(DEL,1)
      Q2=QG2(DEL,2)
      Q3=QG2(DEL,3)
      QPR1=DQ(2)/(2.+DEL)*(Q2-(1.+DEL)*Q1)
      QPR2=DQ(3)/(2.+DEL)*(Q3-(1.+DEL)*Q2)
      FT=1./(SQ*(2.+DEL))*((2.+DEL)/2.*Q1+
     1  2.*DQ(2)*((-2.+DEL)*Q2+(2.+DEL-DEL2*(3.+DEL))*Q1)/
     1  ((2.+DEL)*DEL)+QPR2-(1.+DEL)*QPR1)
      RETURN
    9 CONTINUE
      FT=1./(2.*SQ)*((FM*FM-.75)*ALOG(DEL)+2./DEL)
      RETURN
   11 CONTINUE
      Q1=QG1(Z,1)
      Q2=QG1(Z,2)
      Q3=QG1(Z,3)
      QP1=DQ(2)/Z1*(Q2-Z*Q1)
      QP2=DQ(3)/Z1*(Q3-Z*Q2)
      FT=1./(SQ*Z1)*(Z1/2.*Q1+2.*DQ(2)*(((Z-3.)*Q2-
     1  (ZQ*Z-4.*Z+1.)*Q1)/(ZQ-1.)+QP2-Z*QP1))
      RETURN
      END
CC
      FUNCTION FT1(T)
      COMMON S,M,G
      COMMON/COM1/LC1,LC2,LC3,LC4,LC5
      COMMON/COMXX/XX
      LC1=LC1+1
      FT1=(XX-T-G)*FT(T)
      RETURN
      END
CC
      FUNCTION FT2(T)
      COMMON S,M,G
      COMMON/COM1/LC1,LC2,LC3,LC4,LC5
      COMMON/COMXX/XX
      LC1=LC1+1
      FT2=(XX+T-G)*FT(T)
      RETURN
      END
```

PROGRAM 3

Computes weighted average at square of calculated axial velocities.

	FORTRAN VARIABLE	ANALYTIC VARIABLE	DESCRIPTION
	S	s	
	M	m	
	X	x	Location of propeller plane
	L1		Determine the two values of x_o to be
	L2		used (both values are same)
Input same as 4	A		Lower limit of outer integral
	B		Upper limit of outer integral
	AERR		Absolute error tolerance for oyter integral
	RERR		Relative error tolerance for outer integral
Output	C1		Denominator of Equation (18)

```
      EXTERNAL FX
      COMMON S,W,GGGG
      COMMON/COM11/CW(500,3),A.(3),A22,B4(3),G4(3),
     1   A1G(3),A33(3),EQ(3),P14(3),B31(3),FAC(3)
      COMMON/CONG2/AG22(6,3),BG22(6,3)
      COMMON/COMFT/D4(3),SQ,AMJ
      COMMON/COMF/RRRR,CL,X,XB
      COMMON/COMFX/XX4(4),L1,L2
      COMMON/COM1/LC1,LC2,LC3,LC4,LC5
      DATA XX0/-1.,-.5,B.,.6/
      CALL UERSET(1,LEVL)
      READ(5,901) S,W,X,L1,L2
901   FORMAT(F,I,F,2I)
      READ(5,902) A,B,AERR,RERR
902   FORMAT(4F)
      PI=3.1415927
      SQ=S*S
      CALL GCONST
      C1=FCADRE(FX,A,B,AERR,RERR,ERR,IER)
      WRITE(6,903) C1
903   FORMAT(1X,E14.6)
      END
```

```
      FUNCTION FX(R)
      EXTERNAL F
      COMMON S,M,GGGG
      COMMON/COMG1/CQ(500,3),AQ(3),A2Q,BQ(3),SQ(3),
     1  A1Q(3),A3Q(3),EQ(3),E1Q(3),B3Q(3),FAC(3)
      COMMON/COMG2/AQ22(6,3),BQ22(6,3)
      COMMON/COMFT/DQ(3),SG,AMZ
      COMMON/COMF/RRRR,CL,X,XØ
      COMMON/COMFX/XXØ(4),L1,L2
      COMMON/COM1/LC1,LC2,LC3,LC4,LC5
      IF(ABS(R).GT.1.E-8) GO TO 11
      FX=0.
      GO TO 22
11    CONTINUE
      RRRR=R
      PI=3.1415927
      A=-1.
      B=1.
      AERR=0.
      RERR=.00001
      XØ=XXØ(L1)
      CG1=DCADRE(F,A,B,AERR,RERR,ERR,IER)
      SK1=CG1*(1./(8.*PI*S*SQRT(R*S)))
      XØ=XXØ(L2)
      CG2=DCADRE(F,A,B,AERR,RERR,ERR,IER)
      SK2=CG2*(1./(8.*PI*S*SQRT(R*S)))
      FX=R*SK1*SK2
22    CONTINUE
      RETURN
      END
C
      FUNCTION F(G)
      COMMON S,M,GGGG
      COMMON/COMFT/DQ(3),SG,AMZ
      COMMON/COMF/R,CL,X,XØ
      COMMON/COM1/LC1,LC2,LC3,LC4,LC5
      LC1=LC1+1
      C=1.
      BK=(X-G)*(X-G)
      RK1=(R-S)*(R-S)
      RK2=(R+S)*(R+S)
      BKP=4*R*S*DQ(2)*(S*S-R*R-BK)/((BK+RK1)*(BK+RK2))
      Z=(BK+R*R+S*S)/(2*R*S)
      H=1.
      IF ((-C.LT.G).AND.(G.LE.XØ)) PM=H
      IF ((XØ.LT.G).AND.(G.LT.C)) PM=H*(C-G)/(C-XØ)
      IF (Z.LT.1.09) GO TO 51
      Q1=QQ1(Z,1)
      Q2=QQ1(Z,2)
      GO TO 100
51    CONTINUE
      DEL=Z-1.
      Q1=GQ2(DEL,1)
      Q2=QQ2(DEL,2)
100   F=PM*(-Q1+BKP*(Q2-Z*Q1))
      RETURN
      END
```

PROGRAM 4

Computer h using least square fit between measured and calculated axial velocities.

	FORTRAN VARIABLE	ANALYTIC VARIABLE	DESCRIPTION
	S	S	
	M	m	
	x	x	Location of propeller plane
	L1		Determine the two values of x_o (to be
Input same as 3	L2		[used (both values are the same
	A		Lower limit of outer integral
	B		Upper limit of outer integral
	AERR		Absolute error tolerance for outer integra.
	RERR		Relative error tolerance for outer integral
	AAAA		Denominator of equation (18) (from program 3)
	XXO(L1)		[Two values of x_o used
	XXO(L2)		
	C1		Numerator of Equation (18)
Output	AAAA	ι/C_L	
	HHHH	h	h to give least square fit
	CCLL	C_L	computer from H obtained by this program from Equation (13)

```
      EXTERNAL FX
      COMMON S,M,GGGG
      COMMON/COMG1/CG(500,3),AG(3),A2G,B2(3),G2(3),
     1  A1G(3),A3G(3),BG(3),B1G(3),B3G(3),FAC(3)
      COMMON/COMG2/AG22(6,3),BG22(6,3)
      COMMON/COMFT/DG(3),SG,AMG
      COMMON/COMF/RRRR,CL,X,XG
      COMMON/COMFX/XXG(4),L1,L2
      COMMON/COMGT/RRM(9),UUM(9)
      COMMON/COM1/LC1,LC2,LC3,LC4,LC5
      DATA XXG/-1.,-.5,0.,.6/
      DATA RRM/.1111111,.2222222,.3333333,.4444444,
     1  .5555555,.6666666,.7777777,.8888888,1./
      DATA UUM/.0731,.1548,.2398,.3037,.3316,
     1  .3496,.3532,.3256,.2975/
      CALL UERSET(1,LEVL)
      READ(5,901) S,M,X,L1,L2
901   FORMAT(F,I,F,2I)
      READ(5,902) A,B,AERR,RERR
902   FORMAT(4F)
      READ(5,901) AAAA
      PI=3.1415927
      DO 111 I=1,9
      RRM(I)=S*RRM(I)
111   CONTINUE
      SQ=S*S
      CALL QCONST
      C1=FCADRE(FX,A,B,AERR,RERR,ERR,IER)
      IF(ABS(AAAA).LT.1.E-8) AAAA=1.
      HHHH=C1/AAAA
      CCLL=.25*HHHH*(3.+XXG(L1))
      WRITE(6,903) XXG(L1),XXG(L2),C1
      WRITE(6,903) AAAA,HHHH,CCLL
903   FORMAT(1X,3E14.6)
      END
```

```
      FUNCTION FX(R)              R-2298
      EXTERNAL F
      COMMON S,M,GGGG
      COMMON/COM11/CL(500,3),AQ(3),A2Q,BQ(3),CQ(3),
     1  A1Q(3),A3Q(3),EQ(3),B1Q(3),BBQ(3),FAC(3)
      COMMON/COM22/AQ22(6,3),FG22(6,3)
      COMMON/COMFT/DQ(3),SQ,AMO
      COMMON/COMF/RRRP,CL,X,XC
      COMMON/COMFX/XXJ(4),L1,L2
      COMMON/COM1/LC1,LC2,LC3,LC4,LC5
      IF(ABS(R).GT.1.E-8) GO TO 11
      FX=0.
      GO TO 22
11    CONTINUE
      RRRR=R
      PI=3.1415927
      A=-1.
      B=1.
      AERR=0.
      RERR=.0001
      XC=XXJ(L1)
      CG1=DCADRE(F,A,B,AEPR,RERR,ERR,IER)
      SK1=CG1*(1./(8.*PI*S*SQRT(R*S)))
      SK2=FINTP(RRRR)
      FX=R*SK1*SK2
22    CONTINUE
      RETURN
      END
CC
      FUNCTION F(G)
      COMMON S,M,GGGG
      COMMON/COMFT/DQ(3),SQ,AMO
      COMMON/COMF/R,CL,X,XC
      COMMON/COM1/LC1,LC2,LC3,LC4,LC5
      LC1=LC1+1
      C=1.
      BK=(X-G)*(X-G)
      RK1=(R-S)*(R-S)
      RK2=(R+S)*(R+S)
      BKP=4*R*S*DQ(2)*(S*S-R*R-BK)/((BK+RK1)*(BK+RK2))
      Z=(BK+R*R+S*S)/(2*R*S)
      H=1.
      IF ((-C.LT.G).AND.(G.LE.XC)) PM=H
      IF ((XC.LT.G).AND.(G.LT.C)) PM=H*(C-G)/(C-XC)
      IF (Z.LT.1.09) GO TO 51
      Q1=QQ1(Z,1)
      Q2=QQ1(Z,2)
      GO TO 100
51    CONTINUE
      DEL=Z-1.
      Q1=QQ2(DEL,1)
      Q2=QQ2(DEL,2)
100   F=PM*(-Q1+BKP*(Q2-Z*Q1))
      RETURN
      END
CC
      FUNCTION FINTP(R)
      COMMON/COMDT/RRM(9),UUM(9)
      FINTP=4.*UUM(9)
      DO 1 I=1,9
```

```
      IF(R.GE.RRM(I+1)) GO TO 1
      FINTP=UUM(I)+(R-RRM(I))*(UUM(I+1)-UUM(I))/(RRM(I+1)-
   1    RRM(I))
      GO TO 11
   1  CONTINUE
  11  CONTINUE
      RETURN
      END
```

PROGRAM 5

Calculates associated Legendre Function $Q_{m-1/2}(Z)$ for given m and Z. (Used as subroutine for all foregoing programs.)

```
CC      SUBROUTINE TO COMPUTE CONSTANTS DEPENDING ON  M AND
CC      INPUT TO  Q FUNCTIONS
        SUBROUTINE QCONST
        COMMON S,M,GGGG
        COMMON/COMQ1/CQ(500,3),AQ(3),A2Q,BQ(3),GQ(3),
     1  A1Q(3),A3Q(3),EQ(3),B1Q(3),B3Q(3),FAC(3)
        COMMON/COMQ2/AQ22(6,3),BQ22(6,3)
        COMMON/COMFT/DQ(3),SQ,AMQ
CC
CC      CONSTANTS FOR 1ST  Q  FUNCTION
CC
        A2Q=1.7724539
        FM=M
        DQ(1)=FM-.5
        DQ(2)=FM+.5
        DQ(3)=FM+1.5
        DO 1 I=1,3
        AQ(I)=(DQ(I)+2.)/2.
        BQ(I)=(DQ(I)+1.)/2.
        GQ(I)=DQ(I)+1.5
        A1Q(I)=DQ(I)+1.
        A3Q(I)=DQ(I)+1.5
        EQ(I)=DQ(I)+1.
        CALL GMMMA(A1Q(I),B1Q(I),IER1)
        CALL GMMMA(A3Q(I),B3Q(I),IER3)
        FAC(I)=B1Q(I)*A2Q/((2.**EQ(I))*B3Q(I))
        CQ(1,I)=AQ(I)/GQ(I)
        DO 2 L=2,500
        CQ(L,I)=CQ(L-1,I)*((AQ(I)+L-1.)/(GQ(I)+L-1.))
     2  CONTINUE
     1  CONTINUE
CC
CC      CONSTANTS FOR 2ND  Q  FUNCTION
CC
        DO 3 L=1,3
        N22=DQ(L)+.5
        CQ22=0.
        IF(N22.EQ.0) GO TO 21
        DO 11 I=1,N22
        CQ22=CQ22+1./(2.*I-1.)
     11 CONTINUE
     21 CONTINUE
        AQ22(1,L)=5./2.*ALOG(2.)-2.*CQ22
        BQ22(1,L)=-.5
        DO 40 I=1,5
        NP=I-1
        BQ22(I+1,L)=BQ22(I,L)*(N22**2-1./4.-NP*(NP+1))/
     1  (2.*(NP+1)**2)
        AQ22(I+1,L)=AQ22(I,L)*(N22**2-1./4.-NP*(NP+1))/
     1  (2.*(NP+1)**2)-BQ22(I,L)*(2.*(N22**2-1./4.)+
     1  (NP+1))/(2.*(NP+1)**3)
     40 CONTINUE
     3  CONTINUE
CC
CC      CALCULATION OF  AMQ ,USED BY  FUNCTION  FT
        AM1=0.
        DO 8 K=1,M
        AM1=AM1+1./(2.*K-1.)
     8  CONTINUE
        AMQ=2.5*ALOG(2.)-2.*AM1
        RETURN
        END
```

B-18

```
CC          FIRST  Q  FUNCTION
            FUNCTION QQ1(Z,L)
            COMMON/COMM1/CQ(5,,3),AQ(3),AZ.,BQ(3),SQ(3),
       1     A1Q(3),A3Q(3),BQ(3),B1Q(3),B3Q(3),FAC(3)
            COMMON/COMPT/DQ(5),SQ,AMX
            COMMON/COM1/LC1,LC2,LC3,LC4,LC5
            LC3=LC3+1
            ZF=1./(Z*Z)
            F=FAC(L)/(Z**SQ(L))
            DDD=BQ(L)*F*ZF
            DO 2  I=2,5
            FLI=I
            T=CQ(I-1,L)*DDD
            F=F+T
            IF(ABS(T).LT.J.JJ.JJ1) GO TO 5
            DDD=DDD*ZF*((BQ(L)+FLI-1.)/FLI)
   2        CONTINUE
   5        CONTINUE
            QQ1=F
            RETURN
            END
CC
CC          SECOND  Q  FUNCTION
            FUNCTION QQ2(DEL,L)
            COMMON/COMM22/AQ22(6,3),BQ22(6,3)
            COMMON/COM1/ LC1,LC2,LC3,LC4,LC5
            LC4=LC4+1
            SUM1=0.
            SUM2=0.
            TESTJ1=0.
            TESTJ2=0.
            DO 40 I=1,5
            NP=I-1
            SUM1=SUM1+AQ22(I,L)*DEL**NP
            SUM2=SUM2+BQ22(I,L)*DEL**NP
            TEST1=ABS(SUM1)
            TEST2=ABS(SUM2)
            IF(ABS(TEST1-TESTJ1).GT.0.J0J0JJ1) GO TO 40
            IF(ABS(TEST2-TESTJ2).LT.0.J0J0J01) GO TO 5J
            TESTJ1=TEST1
            TESTJ2=TEST2
   40       CONTINUE
   5J       CONTINUE
            QQ2=SUM1+ALOG(DEL)*SUM2
            RETURN
            END
```
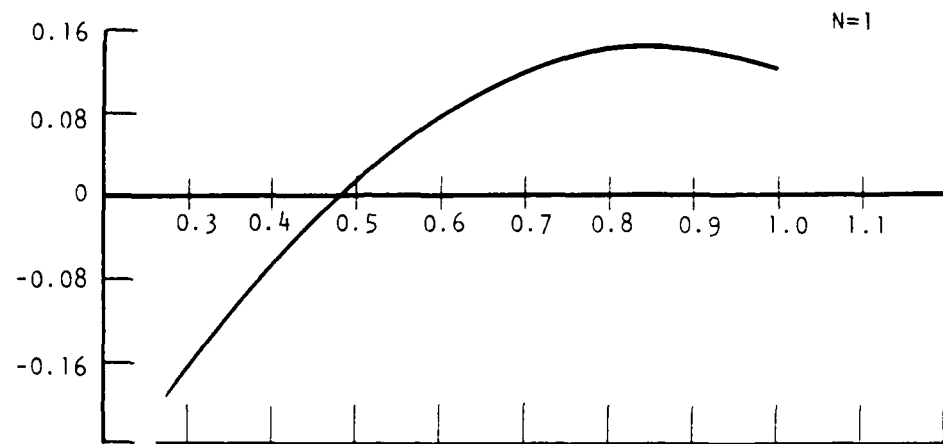
Figure 1.   Radial Variation of Shaft-Frequency Wake Harmonic
            for NSRDC Model 4602 (from Hadler & Cheng SNAME
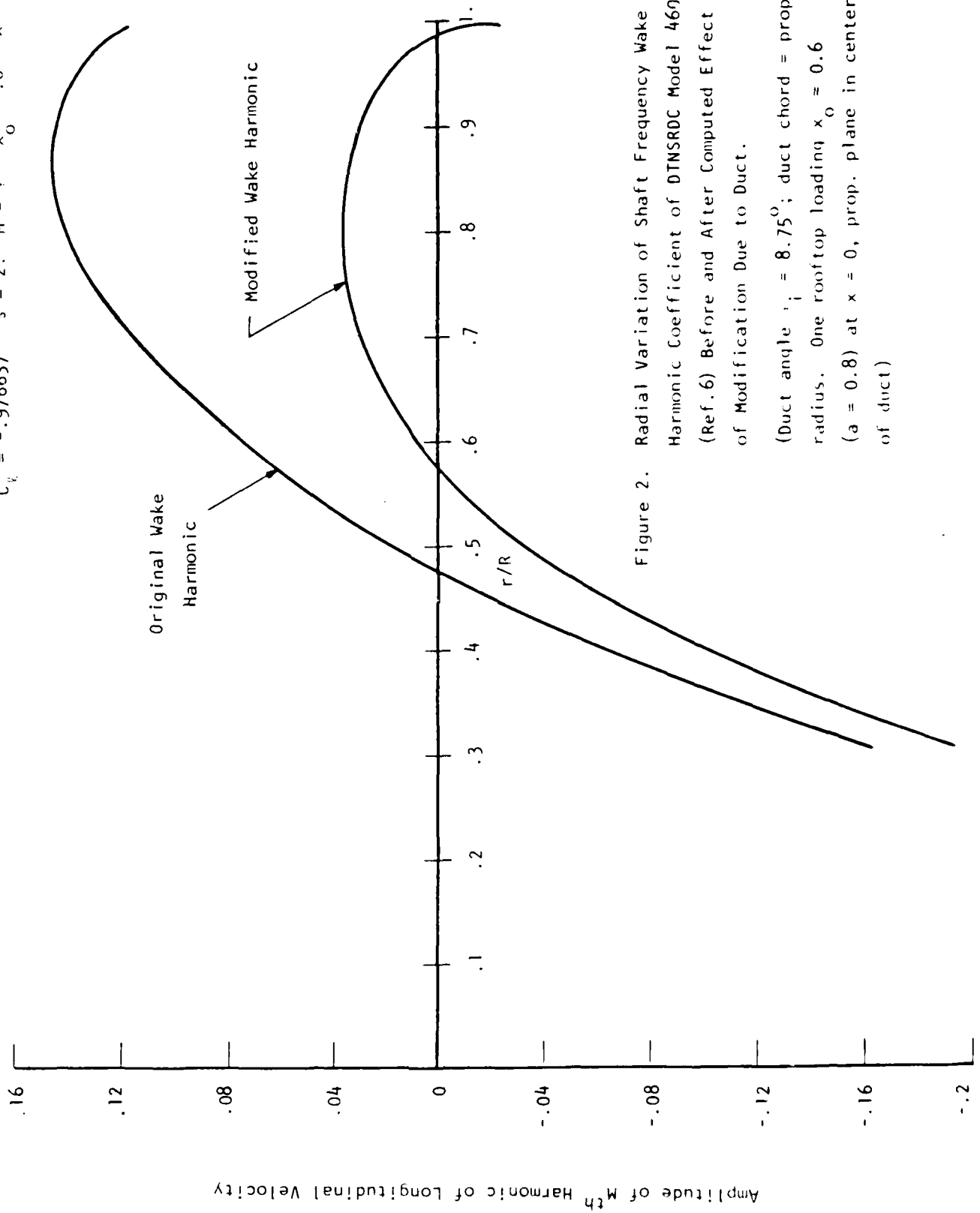   Trans., Vol. 73, 1965)

Figure 2. Radial Variation of Shaft Frequency Wake Harmonic Coefficient of DTNSRDC Model 4602 (Ref.6) Before and After Computed Effect of Modification Due to Duct.

(Duct angle $\eta_i = 8.75^\circ$; duct chord = prop. radius. One rooftop loading $x_o = 0.6$ (a = 0.8) at x = 0, prop. plane in center of duct)
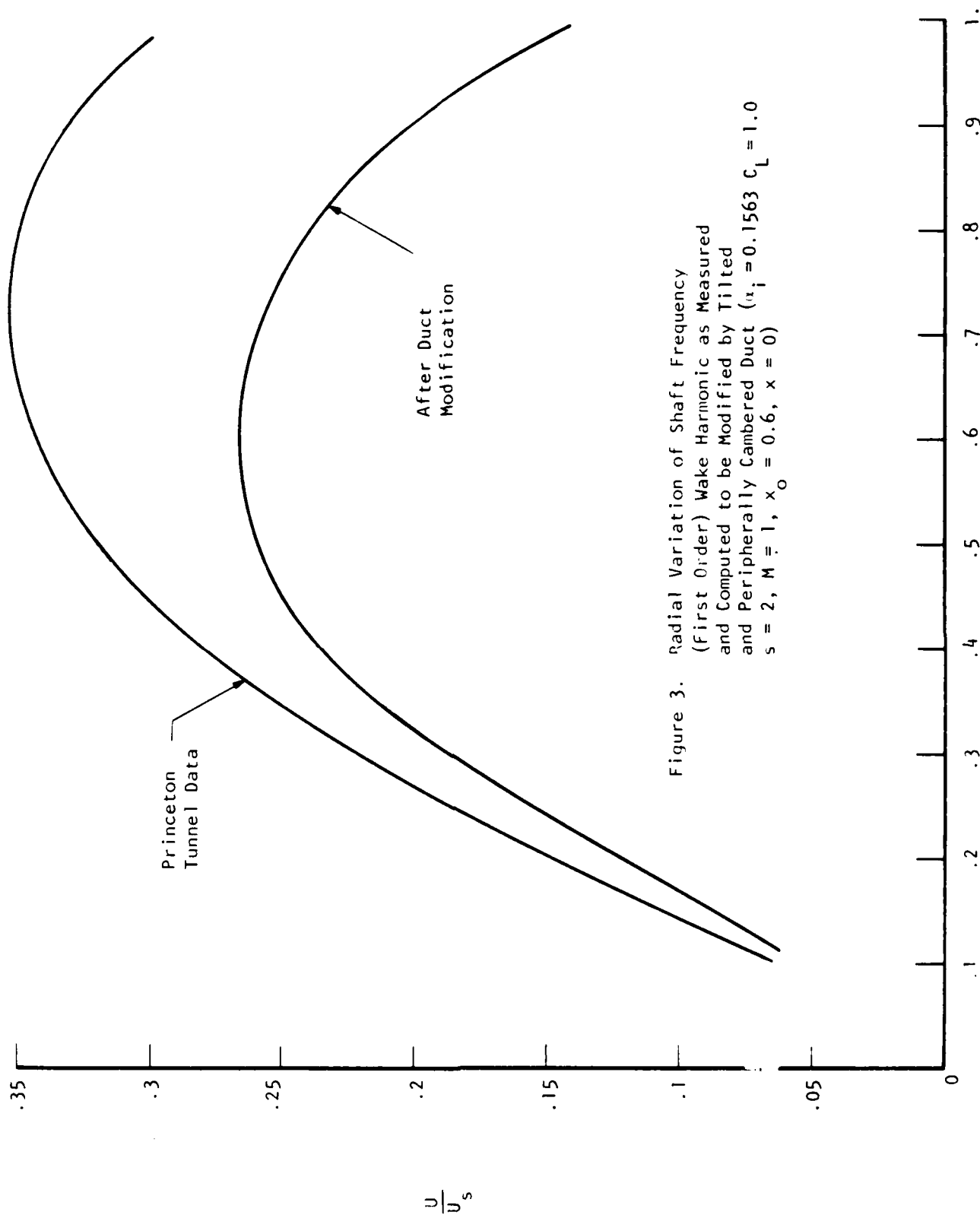
Figure 3. Radial Variation of Shaft Frequency (First Order) Wake Harmonic as Measured and Computed to be Modified by Tilted and Peripherally Cambered Duct ($\alpha_i = 0.1563$ $C_L = 1.0$ $s = 2$, $M = 1$, $x_o = 0.6$, $x = 0$)

FIGURE 4. DUCT CAMBER AMPLITUDE DISTRIBUTION